Inorg. Chem. **2006**, *45*, 8394–8402

Crystal Growth and Structure Determination of Oxygen-Deficient $Sr_6Co_5O_{15}$

Junliang Sun,[†] Guobao Li,[†] Zhaofei Li,[†] Liping You,[‡] and Jianhua Lin*[,†]

Beijing National Laboratory for Molecular Sciences, State Key Laboratory of Rare Earth Materials Chemistry and Applications, College of Chemistry and Molecular Engineering, Peking University, Beijing 100871, China, and Laboratory of Electron Microscopy, Department of Physics, Peking University, Beijing, 100871, China

Received May 18, 2006

Large single crystals of oxygen-deficient $Sr_6Co_5O_{15-\delta}$ compounds, i.e., $Sr_6Co_5O_{14.70}$ and $Sr_6Co_{4.9}Ni_{0.1}O_{14.36}$, were obtained by using K_2CO_3 flux in the presence of additives of transition metal oxides. The single-crystal structure determination shows that the structures of $Sr_6Co_5O_{14.70}$ and $Sr_6Co_{4.9}Ni_{0.1}O_{14.36}$ crystallize in the space group $R\bar{3}$ and can be described as one-dimensional face-sharing CoO_3 polyhedral chains and Sr cation chains. Unlike the other known 2H-perovskite-related oxides in which the polyhedral chains consist of octahedra (Oh) and trigonal prism (TP), the structure of $Sr_6Co_5O_{14.70}$ and $Sr_6Co_{4.9}Ni_{0.1}O_{14.36}$ contain Oh and intermediate polyhedra (IP) and can be attributed to a general structure formula $A_6A'_2B_3O_{15-\delta}$, which is closely related to the known $A_6A'B_4O_{15}$ phases by shifting of a B atom and the O_3 triangle along the *c* axis. Further study on O3 reveals that this oxygen position splits into two independent positions, corresponding to polyhedral geometry of IP and TP, respectively. Therefore, the polyhedral chain in the structure should be more precisely described as a random composite of the 4Oh + TP and 3Oh + 2IP. This model is used to interpret the magnetic properties, although not quantitatively. The 4-D structure analysis was also conducted for both $Sr_6Co_5O_{14.70}$ and $Sr_6Co_{4.9}Ni_{0.1}O_{14.36}$ with a commensurate modulated structure in a 4-D superspace group, $R\bar{3}m(00\gamma)0s$, $\gamma = p/k = 3/5$. By considering the same 4-D superspace group $R\bar{3}m(00\gamma)0s$ but different *t*-phases, one can understand the structure relationship between $Sr_6Co_5O_{14.70}$ and $Sr_6Rh_5O_{15}$.

Introduction

Recently there has been much interest in synthesis and characterization of a large family of oxides structurally related to 2H-perovskite ($BaNiO_3$). The structures of these oxides can be described as a result of alternative stacking of $m[A_3O_9]$ layers and $n[A_3A'O_6]$ layers, followed by filling of the interstitial octahedral B sites. The general formula derived from such stacking is $A_{3n+3m}A'_nB_{3m+n}O_{9m+6n}$ (*m* and *n* are integers), where A is mainly alkaline earth ions, A′ and B can be almost any element from the periodic table, such as alkali,[1,2] alkaline earth,[3,4] transition,[5−20] or main group metal elements.[21,22] Similar to the 2H-perovskite ($BaNiO_3$), the stacking of such layers leads to one-dimensional chains of face-sharing $[A'O_6]$ trigonal prism (TP) and $[BO_6]$ octahedra (Oh) along the *c* axis.[7,23] Numerous oxides of this 2H-perovskite-related family have been synthesized; for instance, $Ca_3Co_2O_6$,[6] $Ba_7PdMn_5O_{18}$,[17] $Ba_8CoRh_6O_{21}$,[18] $Ba_9Rh_8O_{24}$,[19] and $Ba_{11}Rh_{10}O_{30}$[15] are typical compounds, which consist of polyhedral chains repeat of one up nine Oh followed by one TP. The polyhedral chains are well separated

* To whom correspondence should be addressed. E-mail: jhlin@pku.edu.cn. Tel: (8610)62751715. Fax: (8610)62751708.
† College of Chemistry and Molecular Engineering, Peking University.
‡ Department of Physics, Peking University.

(1) Darriet, J.; Grasset, F.; Battle, P. D. *Mater. Res. Bull.* **1997**, *32*, 139.
(2) Claridge, J. B.; Layland R. C.; Adams, R. D.; zur Loye, H.-C. *Z. Anorg. Allg. Chem.* **1997**, *623*, 1131.
(3) Núñez, P.; Trail, S.; zur Loye, H.-C. *J. Solid State Chem.* **1997**, *130*, 35.
(4) Wilkinson, A. P.; Cheetham, A. K. *Acta Crystallogr.* **1989**, *C45*, 1672.
(5) Campá, J. A.; Gutiérrez-Puebla, E.; Monge, M. A.; Rasines, L.; Ruíz-Valero, C. *J. Solid State Chem.* **1994**, *108*, 230.
(6) Fjellvåg, H.; Gulbrandsen, E.; Aasland, S.; Olsen, A.; Hauback, B. C. *J. Solid State Chem.* **1996**, *124*, 190.
(7) Evain, M.; Boucher, F.; Gourdon, O.; Petricek, V.; Dusek, M.; Bezdicka, P. *Chem. Mater.* **1998**, *10*, 3068.
(8) Blake, G. R.; Sloan, J.; Vente, J. F.; Battle, P. D. *Chem. Mater.* **1998**, *10*, 3536.
(9) Claridge, J. B.; Layland, R. C.; Hampton Henley, W.; zur Loye, H.-C. *Chem. Mater.* **1999**, *11*, 1376.
(10) Varela, A.; Boulahya, K.; Parras, M.; González-Calbet, J. M. *Chem. Mater.* **2000**, *12*, 3237.

10.1021/ic060862m CCC: $33.50
Published on Web 09/01/2006

by A cation arrays, which can also be considered as A cation chains. Although the structures of these compounds can be well described in 3-D formalism, they can also be treated as 4-D quasi-composite compounds with two mutually interacting substructures, i.e., the $(A',B)O_3$ chain and the A cation chain.[7,11,15,24] The advantage of the 4-D description is that all of the structures can be described with a uniform small unit cell in the same superspace group $R\bar{3}m(00\gamma)0s$, as well as with less refined variables; this is particularly important for the compounds with large c axis such as $Ba_{11}Rh_{10}O_{30}$. Meanwhile, due to the chainlike structure, they exhibit strong anisotropy in magnetic and electronic properties.[18,19,24]

$Sr_6Co_5O_{15}$ has long been an interesting compound. It was first known as a low-temperature polymorph of the brownmillerite $SrCoO_{3-\delta}$.[25] Extensive efforts had been focused on compositional, structural, and magnetic properties of this phase.[26−35] Only after the structural characterization by Harrison et al.[36] was the stoichiometric nature ($Sr_6Co_5O_{15}$) of this phase established. By using neutron powder diffraction data, they concluded that $Sr_6Co_5O_{15}$ is isostructural with $Sr_6Rh_5O_{15}$ consisting of polyhedral chain repeat of four face-sharing Oh followed by a TP. Very recently, Iwasaki et al.[37] found that, by treating at different temperatures, a series $Sr_6O_5O_{15-\delta}$ with varied stoichiometry up to $\delta = 0.74$ could be obtained. During the years, there has also been a continuing effort of growing single crystals of $Sr_6Co_5O_{15}$ without success. For example, in search of single crystals, Gourdon et al.[38] obtained $Sr_{14}Co_{11}O_{33}$ and $Sr_{24}Co_{19}O_{57}$ instead of $Sr_6Co_5O_{15}$. In comparison with the strontium cobalt oxides that have been obtained as single crystals, such as $Sr_{14}Co_{11}O_{33}$ and $Sr_{24}Co_{19}O_{57}$, the oxidation state of cobalt ions is rather high (+3.6) in $Sr_6Co_5O_{15}$; therefore, a special method is needed in order to obtain single crystals of $Sr_6Co_5O_{15}$.

In the course of investigating possible influence of single-crystal growth of $Sr_6Co_5O_{15}$ by other additives, we found that large single crystals can be obtained for oxygen-deficient $Sr_6Co_5O_{15-\delta}$ in the flux of K_2CO_3 in the presence of small amount of other transition metal oxides (Cr_2O_3, MnO_2, or NiO). Particularly, the single crystals of pure $Sr_6Co_5O_{15-\delta}$ were obtained by using Cr_2O_3 as an additive reagent. Structure characterization using single-crystal diffraction data shows that $Sr_6Co_5O_{15-\delta}$ adopts a similar structure but the space group is $R\bar{3}$ instead of $R32$. The polyhedral chain in the structure can be described as three face-sharing octahedra followed by two heavily distorted polyhedra (intermediate polyhedra). Additionally, analysis of 4-D superspace formalism indicates the structures of $Sr_6Co_5O_{15}$ and $Sr_6Rh_5O_{15}$ are well related; both of them can be described in the same superspace group $R\bar{3}m(00\gamma)0s$ but with different t-phases. The large single crystals also enable us to measure the anisotropic physical properties of $Sr_6Co_5O_{15-\delta}$, which behaves as an antiferromagnetic semiconductor with high conductivity at room temperature.

Experimental Section

Sample Preparation and Crystal Growth. To obtain single crystals of $Sr_6Co_5O_{15}$, we carried out a series of experiments by introducing different additives in the systems. The additives used were transition metal oxides including Cr_2O_3, MnO_2, and NiO. The experiments show that these additives in flux of K_2CO_3 can significantly improve the quality of single crystals. The starting materials, Co_2O_3 (A.R.), $SrCO_3$ (>99.0%), Cr_2O_3 (>99.0%), MnO_2 (A.R.), and NiO (A.R.), were pretreated at 800 (transition metal oxides) and 200 °C ($SrCO_3$), respectively, for 6 h to remove absorbed moisture. A total of 3 g of starting materials in a ratio of Sr/Co/M = 6:5:1 (M = Cr, Mn, or Ni) and about 20 g K_2CO_3 were mixed thoroughly and placed in alumina crucibles. The samples were heated in a rate of 60 °C/h in a furnace to 920 °C and held for 1 week. The furnace was cooled slowly in a rate of 6 °C/h to 850 °C and then switched off, allowing gradual cooling to room temperature. The K_2CO_3 flux was removed by deionized water. At the end, the crystals were sonicleaned in a saturated ammonium chloride solution. The single crystals of hexagonal rodlike or polyhedra shape were obtained as shown in Figure 1. The largest crystal obtained is about 10 mm long and 2 mm in diameter. Powder samples were also prepared by conventional high-temperature solid-state reaction. $SrCO_3$ and Co_2O_3 with a stoichiometric ratio of $Sr_6Co_5O_{15}$ were thoroughly mixed in ethanol and heated at 875 °C in air for 2 weeks with several intermediate

(11) Zakhour-Nakhl, M.; Claridge, J. B.; Darriet, J.; Weill, F.; zur Loye, H.-C.; Perez-Mato, J. M. *J. Am.* Chem. Soc. **2000**, *122*, 1618.
(12) Stitzer, K. E.; Abed, A. E.; Darriet, J.; zur Loye, H. C. *J. Solid State Chem.* **2004**, *177*, 1405.
(13) Davis, M. J.; Smith, M. D.; zur Loye, H.-C. *J. Solid State Chem.* **2003**, *173*, 122.
(14) Abed, A. E.; Gaudin, E.; zur loye, H.-C.; Darriet, J. *Solid State Sci.* **2003**, 5, 59.
(15) Stitzer, K. E.; Abed, A. E.; Darriet, J.; zur Loye, H.-C. *J. Am. Chem. Soc.* **2004**, *126*, 856.
(16) Perez-Mato, J. M.; Zakhour-Nakhl, M.; Weill, F.; Darriet, J.*J. Mater. Chem.* **1999**, *9*, 2795.
(17) Battle, P. D.; Burley, J. C.; Cussen, E. J.; Darriet, J.; Weill, F. *J. Mater. Chem.* **1999**, *9*, 479.
(18) zur Loye, H.-C.; Stitzer, K. E.; Smith, M. D. *Inorg. Chem.* **2001**, *40*, 5152.
(19) Stitzer, K. E.; Smith, M. D.; Darriet, J.; zur Loye, H.-C. *Chem. Commun.* **2001**, 1680.
(20) Campá, J.; Gutiérrez-Puebla, E.; Monge, A.; Rasines, I.; Ruíz-Valero, C. *J. Solid State Chem.* **1996**, *126*, 27.
(21) Carlson, V. A.; Stacy, A. M. *J. Solid State Chem.* **1992**, *96*, 332.
(22) Battle, P. D.; Hartwell, S. J.; Moore, C. A. *Inorg. Chem.* **2001**, *40*, 1716.
(23) Darriet, J.; Subramanian, M. A. *J. Mater. Chem.* **1995**, *5*, 543
(24) Stitzer, K. E.; Abed, A. E.; Darriet, J.; zur Loye, H.-C. *J. Am. Chem. Soc.* **2001**, *123*, 8790.
(25) Grenier, J.-C.; Ghodbane, S.; Demazeau, G.; Pouchard, M.; Hagenmuller, P. *Mater. Res. Bull.* **1979**, *14*(6), 831.
(26) Takeda, Y.; Kanno, R.; Takada, T.; Yamamoto, O.; Takano, M.; Bando, Y. *Z. Anorg. Allg. Chem.* **1986**, 259.
(27) Rodríguez, J.; González-Calbet, J. M. *Mater. Res. Bull.* **1986**, *21*(4), 429.
(28) Battle, P. D.; Gibb, T. C.; Steel, A. T. *J. Chem. Soc., Dalton Trans.* **1987**, *10*, 2359.
(29) Battle, P. D.; Gibb, T. C. *J. Chem. Soc., Dalton Trans.* **1987**, *3*, 667.
(30) Battle, P. D.; Gibb, T. C.; Steel, A. T. *J. Chem. Soc., Dalton Trans.* **1988**, *1*, 83.
(31) Rodriguez, J.; Gonzalez-Calbet, J. M.; Grenier, J. C.; Pannetier, J.; Anne, M. *Solid State Commun.* **1987**, *62*(4), 231.
(32) Bezdicka, P.; Wattiaux, A.; Grenier, J. C.; Pouchard, M.; Hagenmuller, P. *Z. Anorg. Allg. Chem.* **1993**, *619*(1), 7.
(33) Grenier, J. C.; Fournès, L.; Pouchard, M.; Hagenmuller, P. *Mater. Res. Bull.* **1986**, *21*(4), 441.
(34) Takeda, T.; Watanabe, H. *J. Phys. Soc. Jpn.* **1972**, *33*(4), 973.
(35) Takeda, T.; Watanabe, H.; Yamaguchi, Y. *J. Phys. Soc. Jpn.* **1972**, *33*(4), 970.
(36) Harrison, W. T. A.; Hegwood, S. L.; Jacobson, A. J. *J. Chem. Soc., Chem. Commun.* **1995**, 1953.
(37) Iwasaki, K.; Ito, T.; Matsui, T.; Nagasaki, T.; Ohta, S.; Koumoto, K. *Mater. Res. Bull.* **2006**, *41*, 732.
(38) Gourdon, O.; Petricek, V.; Dusek, M.; Bezdicka, P.; Durovic, S.; Gyepesova, D.; Evain, M. *Acta Crystallogr.* **1999**, *B55*, 841.

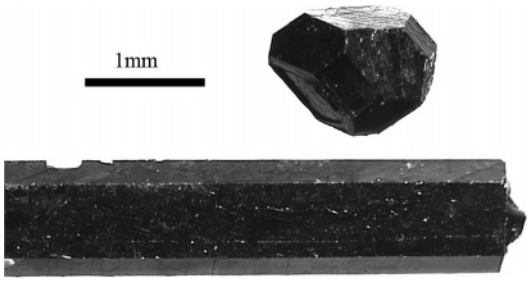

Figure 1. Flux-grown single crystals of $Sr_6Co_5O_{15}$: hexagonal rodlike and polyhedra-shaped.

Table 1. Chemical Analysis of Metal Elements in $Sr_6Co_{5-\delta}M_\delta O_{15}$ Samples

MO_x	Sr (mol %)	Co (mol %)	M (mol %)	formula
Cr_2O_3	54.8	45.2	0.0	$Sr_6Co_5O_{14.70(3)}$
MnO_2	54.2	43.5	2.3	$Sr_6Co_{4.75}Mn_{0.25}O_{15-\delta}$
NiO	54.3	44.8	1.0	$Sr_6Co_{4.9}Ni_{0.1}O_{14.36(6)}$

grindings. The major phase of the product is $Sr_6Co_5O_{15}$, but a trace of Co_3O_4 was always present.[36] A synthesis reaction at high temperature (>950 °C) led to decomposition of $Sr_6Co_5O_{15}$ into other phases. The atomic ratios of metal elements in the crystals were analyzed by using inductively coupled plasma atomic emission spectroscopy (ICP) on a Leeman Labs Profile Spec ICP-AES (Table 1). The single crystals obtained by using Cr_2O_3 as an addictive were found as a pure $Sr_6Co_5O_{15}$ sample, while the MnO_2 and NiO additives yield substituted samples but the content of the substitution is quite low. The oxygen content in this sample was analyzed by using iodometric titration. The nominal formulas of the compounds obtained from chemical analysis are $Sr_6Co_5O_{14.70(3)}$ and $Sr_6Co_{4.9}Ni_{0.1}O_{14.36(6)}$.

Diffraction Data Collection. Single-crystal diffraction data of $Sr_6Co_5O_{14.70}$ and $Sr_6Co_{4.9}Ni_{0.1}O_{14.36}$ were collected on an Enraf-Nonius Kappa CCD diffractometer using Mo Kα radiation (λ = 0.71069 Å). Absorption correction was applied by the numerical method with XRed[39] and XShape[40] or the multiscan method. Data processing and the refinement were performed using both Shelx97[41] and Jana2000[42] program packages. Powder X-ray diffraction data was recorded using a Rigaku D/Max-2000 diffractometer with graphite-monochromatized Cu Kα radiation at 40 kV, 100 mA in the range of 10−120° with step scanning mode.

Indexation of the Diffraction Patterns. Indexation of the diffraction of the single-crystal data yielded a rhombohedral unit cell, a = 9.459(1) Å and c = 12.469(2) Å for $Sr_6Co_5O_{14.70}$ and a = 9.440(1) Å and c = 12.476(3) Å for $Sr_6Co_{4.9}Ni_{0.1}O_{14.36}$. The lattice constants suggested that these single-crystal samples are indeed oxygen deficient and the content of the oxygen vacancies obtained from the correlation curve proposed by Iwasaki et al.[37] agree quite well with the result of chemical analysis. Figure 2 shows the selected area electron diffraction patterns of $Sr_6Co_5O_{14.70}$ ([010] and [1$\bar{1}$0]) and $Sr_6Co_{4.9}Ni_{0.1}O_{14.36}$ ([010] and [001]). The diffraction pattern of $Sr_6Co_{4.9}Ni_{0.1}O_{14.36}$ can be interpreted with the lattice constants of the rhombohedral cell. However, weak super-reflections

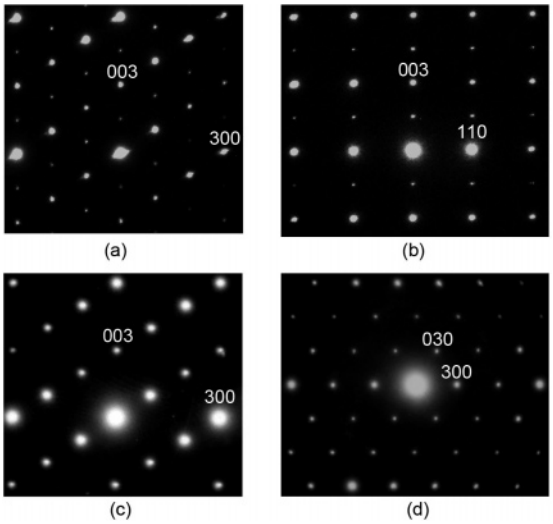

Figure 2. SAED patterns: $Sr_6Co_5O_{14.70}$ along [010] (a) and [1$\bar{1}$0] (b) zone axis; $Sr_6Co_{4.9}Ni_{0.1}O_{14.36}$ along [010] (c) and [001] (d) zone axis.

along the c axis were observed for $Sr_6Co_5O_{14.70}$, as shown in Figure 2a and b, which correspond to a larger rhombohedral cell ($a' = a$, $c' = 2c$), indicative of certain ordering in the structure. These super-reflections can also be detected in the single crystal diffraction data, but they are mostly very weak. Structure refinement with large rhombohedral cell was difficult and unstable; therefore, we focused only on the average structure of $Sr_6Co_5O_{14.70}$ in this paper.

3-D Structure Determination. The analysis of the intensity statistics of the single-crystal diffraction data of $Sr_6Co_5O_{14.70}$ suggested the possible space group of $R\bar{3}$ or $R3$ (R_{sym} = 0.054); this is different from the previous structure determination on a neutron powder diffraction data,[36] where the space group $R32$ and the structure model of $Sr_6Rh_5O_{15}$ were used. The average structure of $Sr_6Co_5O_{14.70}$ was established by the direct method in the space group $R\bar{3}$. Six atomic positions, i.e., one Sr, three Co, and two O, can be readily identified from the direct method (R = 0.13). Including a twining operation of the trigonal lattice (010, 100, 00$\bar{1}$) and anisotropic thermal displacement parameters for the heavy atoms (Sr and Co), the residual value of the refinement reduced to about R = 0.050. At this stage, a half-occupied oxygen position (O3, 3.8e/Å^3) was identified with Co3−O3 distance about 1.85 Å (R = 0.042). This oxygen position has a relatively large thermal parameter (0.077 Å^2), originating possibly from either oxygen vacancies or further disordering of the oxygen atoms. Refining the occupancy factors for all oxygen positions leads to Occ(O3) = 0.43-(3) and an improved thermal parameter (0.066 Å^2). The further refinement with anisotropic temperature factor resulted in an elongated ellipsoid for O3 (R = 0.0388). The composition obtained from structure refinement is $Sr_6Co_5O_{14.6(1)}$, agreeing quite well with that obtained from chemical analysis.

To confirm this structure solution, we also conducted the structure refinements using the structure model of $Sr_6Rh_5O_{15}$ ($R32$).[24] The fitting of the single-crystal data to the $R32$ model is rather poor as far as the residual value (R = 0.074) is concerned. Large residual Fourier peaks (2.9 and −3.51 e/Å^3) were found around Sr positions, indicative of inappropriate assignment of Sr at the special Wyckoff positions (9e and 9d). In addition, the thermal parameters of Sr atoms are quite large in comparison with that in the $R\bar{3}$ model. Obviously, the structure detail of our oxygen deficient crystals, $Sr_6Co_5O_{14.70}$, is significantly different from that of the powder sample in Harrison's study.[37] The structure of $Sr_6Co_{4.9}Ni_{0.1}O_{14.36}$ was determined in a similar way. The final refinement leads to R =

(39) *XRed, data reduction program*, revision 1.02; Stoe and Cie: Darmstadt, Germany, 1996.
(40) *XShape-crystal optimisation for numerical absorption correction*, revision 2.01; Stoe and Cie: Darmstadt, Germany, 1996.
(41) Sheldrick, G. M. *SHELXS-97, Program for crystal structure solution; SHELXL-97, Program for crystal structure refinement*; University of Göttingen: Göttingen, Germany, 1997.
(42) Petricek, V.; Dusek, M.; Palatinus, L. Jana2000; Institute of Physics, Academy of Sciences of the Czech Republic: Praha, Version: 28/05/2001.

Table 2. Crystallographic Data for $Sr_6Co_5O_{14.70}$ and $Sr_6Co_{4.9}Ni_{0.1}O_{14.36}$

formula	$Sr_6Co_5O_{14.70}$	$Sr_6Co_{4.9}Ni_{0.1}O_{14.36}$
fw	1055.57	1050.12
wavelength	Mo K$_\alpha$ (λ = 0.71073 Å)	
space group	$R\bar{3}$	$R\bar{3}$
cell params	a = 9.459(1) Å	a = 9.440(1) Å
	c = 12.469(2) Å	c = 12.476(3) Å
volume	966.1(2) Å^3	962.8(2) Å^3
Z	3	3
density (calcd)	5.443 (g/cm^3)	5.433 (g/cm^3)
abs coeff	30.97 mm^{-1}	31.07 mm^{-1}
twin operation	(010, 100, 00$\bar{1}$)	(100, 010, 00$\bar{1}$)
	0.839/0.161	0.986/0.014
F(000)	1442	1431
$2\theta_{max}$	67°	67°
index ranges	$-11 \le h \le 14$,	$-14 \le h \le 14$,
	$-14 \le k \le 14$,	$-8 \le k \le 14$,
	$-18 \le l \le 14$	$-18 \le l \le 17$
reflns collected	2596	8892
unique reflns	800	814
R(int)	0.0615	0.0459
abs correction	XShape	Multiscan
refinement method	full-matrix least-squares on F^2	
Data/restraints/params	775/0/47	777/0/46
GOF	0.998	1.000
R1($I > 4\sigma(I)$)	0.0388	0.0391
wR2	0.0798	0.0850
$(\Delta/\sigma)_{max}$	<0.001	<0.001

Table 3. Atomic Coordinates in the Structures of $Sr_6Co_5O_{14.70}$ and $Sr_6Co_{4.9}Ni_{0.1}O_{14.36}$ (3-D)

atom	site	x	y	z	U_{eq}(Å^2) [a]	Occ
			$Sr_6Co_5O_{14.70}$			
Sr	18f	0.33186(8)	0.01971(7)	0.08120(6)	0.0147(1)	1
Co1	3b	0	0	0	0.0091(3)	1
Co2	6c	0	0	0.1927(1)	0.0094(2)	1
Co3	6c	0	0	0.6077(1)	0.0173(3)	1
O1	18f	0.1532(5)	0.1615(5)	0.0946(4)	0.0128(8)	1
O2	18f	0.1559(6)	0.1545(6)	0.7121(4)	0.0163(9)	1
O3	18f	−0.064(5)	−0.159(2)	0.495(2)	0.066(8)	0.43(2)
			$Sr_6Co_{4.9}Ni_{0.1}O_{14.36}$			
Sr	18f	0.33223(6)	0.02053(6)	0.08092(4)	0.0098(1)	1
Co1	3b	0	0	0	0.0053(3)	1
Co2	6c	0	0	0.19193(9)	0.0057(2)	1
Co3	6c	0	0	0.6086(1)	0.0137(3)	1
O1	18f	0.1544(4)	0.1624(5)	0.0944(3)	0.0079(6)	1
O2	18f	0.1576(5)	0.1548(5)	0.7125(3)	0.0113(7)	1
O3	18f	−0.074(4)	−0.156(2)	0.499(1)	0.047(6)	0.36(2)

[a] Displacement factor: Isotropic: $U_{eq}=1/3\sum_i\sum_j U^{ij}a_i^*a_j^*\mathbf{a_i}\cdot\mathbf{a_j}$ and anisotropic: $-2\pi^2\sum_i\sum_j U^{ij}a_i^*a_j^*\mathbf{h_i}\cdot\mathbf{h_j}$.

Table 4. Selected Distances in the Structures of $Sr_6Co_5O_{14.70}$ and $Sr_6Co_{4.9}Ni_{0.1}O_{14.36}$ (3-D and 4-D)

	3-D model	4-D model	3-Dmodel	4-D model
Co1−Co2(×2)	2.402(2)	2.399(1)	2.394(1)	2.394(1)
Co2−Co3(×2)	2.489(2)	2.492(3)	2.488(2)	2.490(1)
Co3−Co3(×1)	2.686(3)	2.687(3)	2.711(3)	2.709(2)
Co1−O1(×6)	1.900(4)	1.888(18)	1.904(4)	1.905(9)
Co2−O1(×6)	1.927(5)	1.914(18)	1.929(4)	1.928(9)
Co2−O2(×6)	1.887(5)	1.880(14)	1.896(4)	1.900(7)
Co3−O2(×3)	1.961(5)	1.955(14)	1.963(4)	1.967(11)
Co3−O3 (×3)	1.84(2)	1.84(3)	1.849(15)	1.859(17)
Co3−O3 (×3)	1.92(2)	1.89(3)	1.872(16)	1.886(17)

0.0391 in the space group $R\bar{3}$ with the occupancy 0.36(2) for O3. Table 2 lists the crystallographic information of these two compounds. The atomic coordinates and selected bond distances are listed in Table 3 and Table 4.

Magnetic and Resistance Measurements. Magnetic susceptibility as a function of temperature was performed on a Quantum Design MPMS XL-5 SQUID system equipped with a horizontal rotator sample holder at an applied field of 1 kOe. For measuring powder magnetic susceptibility, crystals of $Sr_6Co_5O_{14.70}$ were ground and placed in a gelatin capsule fastened in a plastic straw for immersion into the SQUID. For measuring the anisotropic susceptibility, a hexagonal rodlike $Sr_6Co_5O_{14.70}$ crystal (about 15 mg) was carefully mounted on a plastic straw on the SQUID, and the orientation of the crystal was estimated by searching the maximum during the rotation. The resistance of $Sr_6Co_5O_{14.70}$ crystal was measured on a hexagonal rodlike crystal in a temperature range from 300 to 100 K using the standard four-probe technique on a Quantum Design PPMS-9T.

Results and Discussion

Crystal Growth. K_2CO_3 was proved to be a promising flux that has been used extensively for growing single crystals of 2H-perovskite-related compounds. However, attempts of using this flux to grow single crystals of $Sr_6Co_5O_{15}$ were not successful. An experiment carried out at 1100 °C in the flux of K_2CO_3 led to formation of small single crystal of $Sr_{14}Co_{11}O_{33}$.[38] On the other hand, according to our experience and references,[36,37] the powder $Sr_6Co_5O_{15}$ sample can only be obtained at about 875 °C, and at higher temperature, other phases are formed. Therefore, we chose the temperature range 920−850 °C for the crystal growth (K_2CO_3 mp = 890 °C). Under such conditions, the $Sr_6Co_5O_{15}$ phase was indeed formed, but in polycrystalline form together with other unknown phases in the flux.

The addition of other transition metals in the flux was initially aimed at the substituted $Sr_6Co_5O_{15}$ crystals. A series of experiments were carried out by using Cr_2O_3, MnO_2, Fe_2O_3, NiO, CuO, or ZnO as the additives. It turned out large single crystals were formed when Cr_2O_3, MnO_2, or NiO was present in the flux. As shown in Table 1, a small amount of Mn and Ni can be substituted in $Sr_6Co_5O_{15}$; however, no Cr was found in the crystals obtained from the Cr_2O_3-containing system. We do not know the exact reaction mechanism and roles of these transition metal ions in the reaction system. However, we did observe the presence of high-oxidation ions in the alkaline flux. The color of filtrate was yellow (containing CrO_4^{2-}) for the Cr system and purple (containing MnO_4^-) for the Mn system. The presence of chromate and permanganate ions was further evidenced by characteristic color change of the transition metal ions. When $H_2C_2O_4$ aqueous solution was added to the filtrate, the solution becomes green for the Cr system (Cr^{3+}) and colorless (Mn^{2+}) for the Mn system. A reasonable paraphrase is that the chromate and permanganate ions may catalyze the redox reaction in the flux, which in turn improves the dissolution and growth of crystals and eventually good shaped large single crystals were formed. In the Ni-contained system, the color of the filtrate was similar with the pure Sr−Co−O system, although single crystals were formed.

3-D Average Structure of $Sr_6Co_5O_{15-\delta}$. Similar to $Sr_6Rh_5O_{15}$, the structure of $Sr_6Co_5O_{14.70}$ can be expressed as two kinds of chains along the c axis, i.e., the CoO_3 polyhedra chains and Sr cation chains, as shown in Figure 3. However, the structure detail of the cobalt polyhedra chain in $Sr_6Co_5O_{14.70}$ is different from that of $Sr_6Rh_5O_{15}$; it consists of three Oh followed by two heavily distorted polyhedra, instead

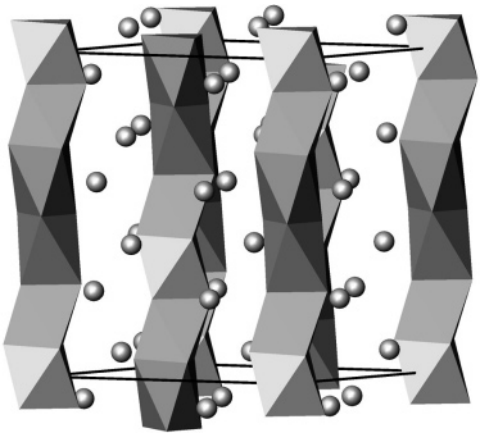

Figure 3. Structure of $Sr_6Co_5O_{14.70}$: the light polyhedra are cobalt octahedra (Oh) and the dark ones are intermediate polyhedra (IP); the strontium ions are represented by bright spheres.

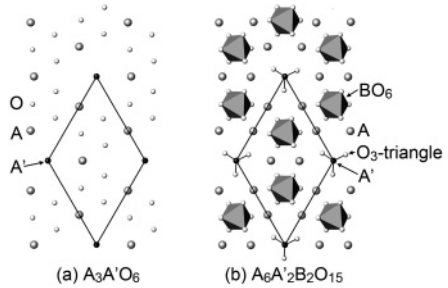

Figure 4. (a) $[A_3A'O_6]$ layer derived by replacing O_3 triangles with A′ atoms in the $[A_3O_9]$ layer; (b) a $[A_6A'_2B_2O_{15}]$ sheet formed by two $[A_3A'O_6]$ layers, where the octahedral sites are occupied by B atoms and O_3 triangles are inserted between the A′ atoms.

of four Oh and one TP in $Sr_6Rh_5O_{15}$. The heavily distorted polyhedron is characterized by the intermediate rotation angle (∼30°) of the two opposite oxygen triangular faces, which is just between the Oh and the TP; therefore, it cannot be assigned as either Oh or TP but is best described as an IP between Oh and TP. In fact, similar intermediate polyhedron was also observed in $Ba_{12}Rh_{9.25}Ir_{1.75}O_{33}$,[12] in which the polyhedral chain consists of eight Oh followed by three IP. In the structure of $Sr_6Co_5O_{14.70}$, the strontium atoms are located in a site of nine-coordinated irregular polyhedron with $d_{av}[Sr-O] = 2.65$ Å. Co1 and Co2 are all octahedrally coordinated by oxygen atoms with $d_{av}[Co1-O] = 1.90$ Å and $d_{av}[Co2-O] = 1.93$ Å. Co3, however, is located at the center of the IP formed by O2 and O3 with average Co3−O distance of about 1.96 Å for O2 and 1.88 Å for O3. The Co−Co distances in the structure vary along the polyhedra chains, $d[Co1-Co2] = 2.402(2)$ Å between the Oh, $d[Co2-Co3] = 2.489(2)$ Å between the Oh and IP, and $d[Co3-Co3] = 2.686(3)$ Å between the IP.

It is known that the structure of $Sr_6Rh_5O_{15}$ can be described as alternative stacking of $[A_3O_9]$ and $[A_3A'O_6]$ layers followed by filling of the interstitial octahedral B sites. Such stacking results in a polyhedral chain consisting of four face-sharing Oh and one TP. As far as the component layers are concerned, the structure of $Sr_6Co_5O_{14.70}$ contains only the $[A_3A'O_6]$ layers. In Figure 4a, we show the $[A_3A'O_6]$ layer derived by replacing an O_3 triangle with an A′ atom in a $[A_3O_9]$ layer. To construct the $Sr_6Co_5O_{14.70}$ structure, we

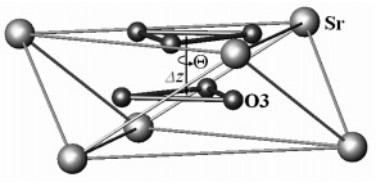

Figure 5. Schematic view of the rotation of O_3 triangle along with the shift in the z direction; Θ represents the rotation angle of O_3 triangle in comparison with that in the $[A_3O_9]$ layer; Δz represents the shift of O_3 triangle along the c axis.

could first stack two such $[A_3A'O_6]$ layers and then rotate one of the layers 60°. Between the layers, the octahedral sites are filled by Co atoms, while O_3 triangles (O3) are inserted between the two opposite A′ atoms to form a $[A_6A'_2B_2O_{15}]$ sheet, as shown in Figure 4b. Since the O_3 triangle (O3) between the opposite A′ atoms is located at the midpoint of two A′ atoms, the orientation of the O_3 triangle differs by 30° from that in the $[A_3O_9]$ layer, as shown in Figure 5, thus to maximize the interaction with the surrounding Sr atoms. In the structure of $Sr_6Co_5O_{14.70}$, the $[A_6A'_2B_2O_{15}]$ sheets stack one over the other along the c axis in a rhombohedral fashion, between which an additional Co atom is added to the octahedral site to complete the structure of $Sr_6Co_5O_{15}$ ($A_6A'_2B_3O_{15}$). On the other hand, the structure of $Sr_6Co_5O_{14.70}$ is related to and can be derived from that of $Sr_6Rh_5O_{15}$ by shifting the O_3 triangle and B atom along the c axis.

In many 2H-perovskite-related oxides, the O_3 triangles may not be exactly located within the $[A_3O_9]$ plane but shift slightly along the c axis, which, in turn, induce rotation of the O_3 triangles, as shown in Figure 5. Two structure parameters, $2\Delta z/c_{perov}$ and Θ, can be used to characterize this type of structure change. As shown in Figure 5, Θ is a rotation angle of the O_3 triangle relative to that in the $[A_3O_9]$ plane. $2\Delta z/c_{perov}$ represents the relative shift of the O_3 triangle along the c axis, where Δz is the change of the z parameter and c_{perov} is the lattice constant of the hexagonal perovskite. For a case of ideal TP, Θ = 0°, for an ideal intermediate polyhedron (IP), Θ = 30°. The Θ values for some typical 2H-perovskite-related oxides are, for example, 7.1° for $Ca_3Co_2O_6$, 6.8° for Sr_3NiRhO_6, 3.3° for $Sr_4Mn_2NiO_9$, 2.7° for $Sr_6Rh_5O_{15}$, 23° for $Sr_6Co_5O_{14.70}$, and 28° for $Sr_6Co_{4.9}Ni_{0.1}O_{14.36}$. In Figure 6, we show a plot of rotation angles (Θ) against $2\Delta z/c_{perov}$ for a few known 2H-perovskite-related oxides,[5,6,7,19,24,36,43] as well as $Sr_6Co_5O_{14.70}$ and $Sr_6Co_{4.9}Ni_{0.1}O_{14.36}$. Although some data are scattered, one can still see the correlation between Θ and $2\Delta z/c_{perov}$. The compounds on the left (small Δz) are close to the ideal trigonal prism cases; thus, the polyhedral chain can be described as Oh and TP. Meanwhile, the compounds on the right (large Δz) consist of heavily distorted polyhedra, which are best described as IP. The correlation between these two simple structure parameters implies that the distortion of the polyhedra is common for most of the 2H-perovskite-related oxides. The IP observed in the structure of $Sr_6Co_5O_{14.70}$ and $Sr_6Co_{4.9}Ni_{0.1}O_{14.36}$ can be considered as an extreme case of the distortion.

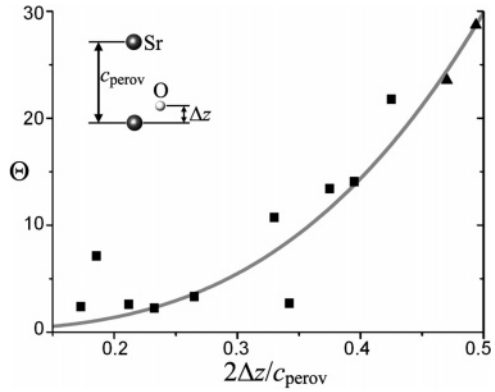

Figure 6. Mapping of the rotation angle (Θ) and relative shift ($2\Delta z/c_{perov}$) of the O_3 triangle relative to the surrounding Sr atoms; the compounds included are $Sr_9Ni_7O_{21}$, $Ca_3Co_2O_6$, $Sr_4Ni_3O_9$, $Ba_6Ni_5O_{15}$, $Sr_6Co_5O_{15}$, $Sr_6Rh_5O_{15}$, $Ba_9Rh_8O_{24}$, and $Ba_{12}Rh_{9.25}Ir_{1.75}O_{33}$ (■), as well as $Sr_6Co_5O_{14.70}$ and $Sr_6Co_{4.9}Ni_{0.1}O_{14.36}$ (▲).

Random Composite Model for $Sr_6Co_5O_{15-\delta}$. The anisotropic temperature factor of O3 exhibits as a long ellipsoid for $Sr_6Co_5O_{14.70}$ and $Sr_6Co_{4.9}Ni_{0.1}O_{14.36}$, indicative of possible splitting of this position. As shown in Table 5, the O3 position can be well described by two independent atoms in the space group $R\bar{3}$ with improved isotropic temperature factors. An interesting observation is that the refined coordinates of O31 and O32 are very similar for both $Sr_6Co_5O_{14.70}$ and $Sr_6Co_{4.9}Ni_{0.1}O_{14.36}$. The corresponding rotation angle is about 30° (O31) and 6° (O32) in $Sr_6Co_5O_{14.70}$ and, about 33° (O31) and 9° (O32) $Sr_6Co_{4.9}Ni_{0.1}O_{14.36}$, which represent, respectively, the geometry of an IP (∼30°) and a TP (∼0°). As far as the polyhedral chain is concerned, the former (O31) corresponds to the polyhedral chain consisting of three Oh and two IP (3Oh + 2IP), while the later (O32) represents the polyhedral chain consisting of four Oh and one TP (4Oh + TP). Therefore, the polyhedral chains in these two compounds can be considered as a random composite of these two types of chain components. The ratio of these two-chain components can be estimated by the refined occupation factors of O31 and O32 (Table 5). One can see that the 4Oh + TP component in the polyhedral chain increases as the decrease of the oxygen vacancies. This result may help us to understand the different structure model in Harrison's study.[36] They were using a powder sample in their experiment, and according to the Iwasaki's study,[37] the stoichiometry of $Sr_6Co_5O_{15-\delta}$ depends strongly on the conditions of heating treatments. For a stoichiometric $Sr_6O_5O_{15}$ sample, one could expect predominance of 4Oh + TP in the structure.

4-D Superspace Formalism Approach. As indicated, $Sr_6Co_5O_{15-\delta}$ crystallizes in the 3-D space group $R\bar{3}$ and the structure is featured in polyhedral chains consisting of three Oh and two IP. On the other hand, the structure of $Sr_6Co_5O_{15-\delta}$ is related to that of $Sr_6Rh_5O_{15}$ (*R*32) by shifting the O_3 triangle along the *c* axis. To establish a symmetry relationship for these two related structure types, one could consider 4-D superspace formalism, since these two 3-D space groups can be considered as the subgroups of a 4-D superspace group by choosing different *t*-phases. The 4-D structure description of 2H-perovskite-related oxides of $A_{3n+3m}A'_nB_{3m+n}O_{9m+6n}$ have been well established as two mutually interacting substructures, i.e., the $(A',B)O_3$ chain with an average c_1 close to $c_{perov}/2$ and the A cation chain with $c_2 = c_{perov}$.[7,11,15,24] For $Sr_6Rh_5O_{15}$, the 4-D structure can be described in the superspace group $R\bar{3}m(00\gamma)0s$ with a rational fraction $\gamma = p/k = 3/5$ ($t = 1/4$), where the *t* is the original phase along the fourth dimension and the value of $t = 1/4$ means the corresponding 3-D section is through a 2-fold axis. The structure of $Sr_6Co_5O_{14.70}$ may also be described in the 4-D superspace group $R\bar{3}m(00\gamma)0s$ with $\gamma = p/k = 3/5$, but with a different *t*-phase. Table 7 summarizes all possible 3-D sections and corresponding space groups of $R\bar{3}m(00\gamma)0s$.[16] For the $R\bar{3}$ space group, the only possible *t*-phase is zero, which means the 3-D section is at the inverse center. The structure can be refined nicely with the 4-D commensurate modulated model in $R\bar{3}m(00\gamma)0s$, $\gamma = p/k = 3/5$ and $t = 0$ with the residual value of $R = 0.060$ for $Sr_6Co_5O_{14.70}$ and $R = 0.064$ for $Sr_6Co_{4.9}Ni_{0.1}O_{14.36}$ using Jana2000. Tables 6 and 7 list the crystallographic data and atomic parameters for the 4-D description of these two structures. (Atomic parameters of $Sr_6Co_{4.9}Ni_{0.1}O_{14.36}$ are listed in the Supporting Information.) To confirm the chosen *t*-phase, these 4-D structures were also refined with $t = 1/4$. The poor fitting of the refinements, i.e., $R = 0.14$ for Sr_6-

Table 5. Splitting of O3 Atoms in the Structure of $Sr_6Co_5O_{14.70}$ and $Sr_6Co_{4.9}Ni_{0.1}O_{14.36}$

compound	atom	*x*	*y*	*z*	U_{eq}(Å^2)	Occ	Θ	TP(%)
$Sr_6Co_5O_{14.70}$	O31	0.161(3)	0.080(4)	0.000(2)	0.023(5)	0.237(7)	30	44
	O32	0.153(4))	0.135(4)	−0.016(2)	0.023(7)	0.19(2)	6	
$Sr_6Co_{4.9}Ni_{0.1}O_{14.36}$	O31	0.158(2)	0.072(3)	0.002(2)	0.013(4)	0.235(7)	33	36
	O32	0.151(4)	0.126(5)	−0.013(2)	0.013(7)	0.13(1)	9	

Table 6. 4-D Refinement for $Sr_6Co_5O_{14.70}$ and $Sr_6Co_{4.9}Ni_{0.1}O_{14.36}$

chemical formula	$Sr_6Co_5O_{14.70}$	$Sr_6Co_{4.9}Ni_{0.1}O_{14.36}$
superspace group	$R\bar{3}m(00\gamma)0s$ ($\gamma = 3/5$)	$R\bar{3}m(00\gamma)0s$ ($\gamma = 3/5$)
W-matrix	$W_2 = (1000, 0100, 0001, 0010)$	
cell params	$a = 9.459(1)$ Å	$a = 9.440(1)$ Å
	$c_1 = 2.494(4)$ Å	$c_1 = 2.495(5)$ Å
twin operation	(010, 100, 00$\bar{1}$)	(100, 010, 00$\bar{1}$)
	(0.841/0.159)	(0.949/0.051)
overall *R* factors	0.0600, 0.1069	0.0623, 0.0773
R factors for main reflns	0.0568, 0.1096	0.0639, 0.0928
R factors for satellites of order 1	0.0691, 0.1111	0.0671, 0.0689
R factors for satellites of order 2	0.0503, 0.0723	0.0467, 0.0470

Table 7. Atomic Coordinates in the Structure of $Sr_6Co_5O_{14.70}$ (4-D)

atom	x_0	y_0	z_0	U_{eq}(Å^2)	$\hat{x}_4$	Δ	amplitude
Co1	0	0	0	0.012(1)	0	0.5	0.15
O	0.151(2)	0.151(2)	0.5	0.016(2)	0.25	0.4	0.10
O3	0.157(3)	0.093(7)	0.515(13)	0.07(2)	0	0.1	0
Sr	1/3	0	1/4	0.0189(3)			
Co			$z_{sin1} = -0.167(1)$				
O			x_{sin1}=0.006(3), $x_{cos1} = -0.0029(5)$, $z_{cos1} = 0.169(3)$				
Sr			$x_{sin1} = -0.01055(6)$, $x_{sin2} = 0.00508(7)$, $z_{sin3} = -0.0066(3)$				
Co			$U_{11cos1} = -0.0134(16)$, $U_{33cos1} = -0.0106(35)$				
Sr			$U_{11sin1} = 0.0017(3)$, $U_{13sin1} = -0.0049(4)$, $U_{11sin2} = 0.0009(4)$, $U_{13sin2} = -0.0017(4)$,				

$Co_5O_{14.70}$ and $R = 0.23$ for $Sr_6Co_{4.9}Ni_{0.1}O_{14.36}$, unambiguously shows that $t = 0$ is the right choice.

It is worth noting that the O3 in the 3-D structure model behaves differently from other oxygen atoms, O1 and O2, in the partial occupancy and the temperature factors, so it was represented by an independent oxygen position in the 4-D structure model. A similar strategy was applied for the $Sr_6Rh_5O_{15}$ where two transition metal sites represent the metal atoms in TP and Oh, respectively. The sawtooth functions were used to fit the modulated wave for cobalt and oxygen sites, and due to the unstability of the refinement, we fixed the amplitude of sawtooth function manually at 0.15 for Co and 0.1 for O. Similar to the 3-D model, the O3 atom has a large thermal parameter (0.07 Å^2 for $Sr_6Co_5O_{14.70}$ and 0.05 Å^2 for $Sr_6Co_{4.9}Ni_{0.1}O_{14.36}$). The same 4-D space group $R\bar{3}m(00\gamma)0s$ with different t-phases for $Sr_6Rh_5O_{15}$ and $Sr_6Co_5O_{15-\delta}$ implies symmetry relationship between these two typical structure types. From the structure refinement, one can calculate the atomic positions in the real space. The factional coordinates for the ith atoms in the υth subsystem are given by

$$\mathbf{r}_{\upsilon i} = \mathbf{r}^0_{\upsilon i} + f_{\upsilon i}(x_4)$$

where $\mathbf{r}^0_{\upsilon i}$ is the average atomic position and $x_4 = \mathbf{q}_\upsilon(\mathbf{n}_\upsilon + \mathbf{r}^0_{\upsilon i}) + t_0$, with $\mathbf{n}_\upsilon$ being integers representing the 3-D lattice vector and t_0 being the original t-phase. $f_{\upsilon i}(x_4)$ is a periodic function with period of 1 which can usually be expanded by Fourier series, and here we expanded it as a sawtooth function as we discussed before. Writing $x_4 = \mathbf{q}_\upsilon \cdot \mathbf{r}^0_{\upsilon i} + (\mathbf{q}_\upsilon \mathbf{n}_\upsilon + t_0) = \mathbf{q}_\upsilon \cdot \mathbf{r}^0_{\upsilon i} + t$, one can draw $\mathbf{r}_{\upsilon i}$ as a function of t, as shown in Figure 7 (only the z component). With $t_0 = 0$, the appropriate t values should be $t_0 + n\gamma$, which are 0, 0.6, 1.2, 1.8, 2.4, 3.0, etc., when going through the subcells. The periodicity of the function allows us to have a complete description in $0 \le t \le 1$.[44] The solid lines in Figure 7 represent the modulation of the Co and O atoms in the 4-D description. The filled or open circles in the figure correspond to the atomic positions in the 3-D description. All points are located at the crosses of the modulation curves and allowed t values (dashed lines) further demonstrating identity of the 3-D and 4-D structure models.

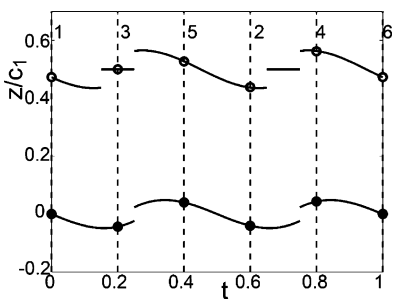

Figure 7. Modulated waves of $Sr_6Co_5O_{14.70}$: two curves represent the modulation wave of Co (down) and oxygen (up) in the 4-D structure. The dashed vertical lines represent the allowed t-phases in different subcells. The circles represent the atomic positions of cobalt (filled) and oxygen (open) in the 3-D structure.

Magnetism and Conductivity. The structure of $Sr_6Co_5O_{14.70}$ is highly anisotropic; thus, one would expect anisotropic magnetic and conductive properties. With availability of large single crystals, we are able to measure orientated magnetic susceptibility and the conductivity along the c axis on a single-crystal sample. Figure 8a shows magnetic susceptibility of a finely ground single-crystal sample for $Sr_6Co_5O_{14.70}$. The susceptibility shows a maximum at about 25 K, followed by a decrease, indicative of antiferromagnetic interactions among the cobalt ions along the polyhedral chains. The origination of the small rise at lower temperature (~5 K) is not clear, but it may come from the imperfections in the crystals that give rise to trace paramagnetic cobalt ions. The inverse of the magnetic susceptibility is linear and follows the Curie−Weiss law above 70 K. The obtained Curie and Weiss constants are $C_m = 3.88$ emu·K·mol^{-1} and $\theta = -25$ K, corresponding to about 5.6 μ_B per formula. The magnetic susceptibility measured on a single crystal (Figure 8b) exhibits a similar behavior parallel to the c axis (χ), but is flat for $\chi_\perp$, indicating that the contribution perpendicular to c axis is rather small. A similar strong anisotropic phenomenon was also observed for $Sr_6Rh_5O_{15}$. Figure 8c shows the $\chi/\chi_\perp$ ratio as a function of temperature. The anisotropy of susceptibility persists all the way up to room temperature and beyond but shows a maximum at about 25 K. On the basis of the crystal structure, we expect that the antiferromagnetic interaction originates mainly from coupling of the cobalt ions along the polyhedral chains. The interchain magnetic interaction might be relatively weak, as indicated by the anisotropy curve of the susceptibility (Figure 8c). In Figure 8b, we also include the magnetic susceptibility of the powder sample and that calculated from the single-crystal susceptibility by using $\chi_{cal} = 1/3\chi + 2/3\chi_\perp$. The two curves overlay quite well, demonstrating that the powder value is well represented for random orientation of single crystals.

(43) Abraham, F.; Minaud, S.; Renard, C. *J. Mater. Chem.* **1994**, *4*(11), 1763.
(44) Van Smaalen, S. *Cryst. Rev* **1995**, *4*, 79.

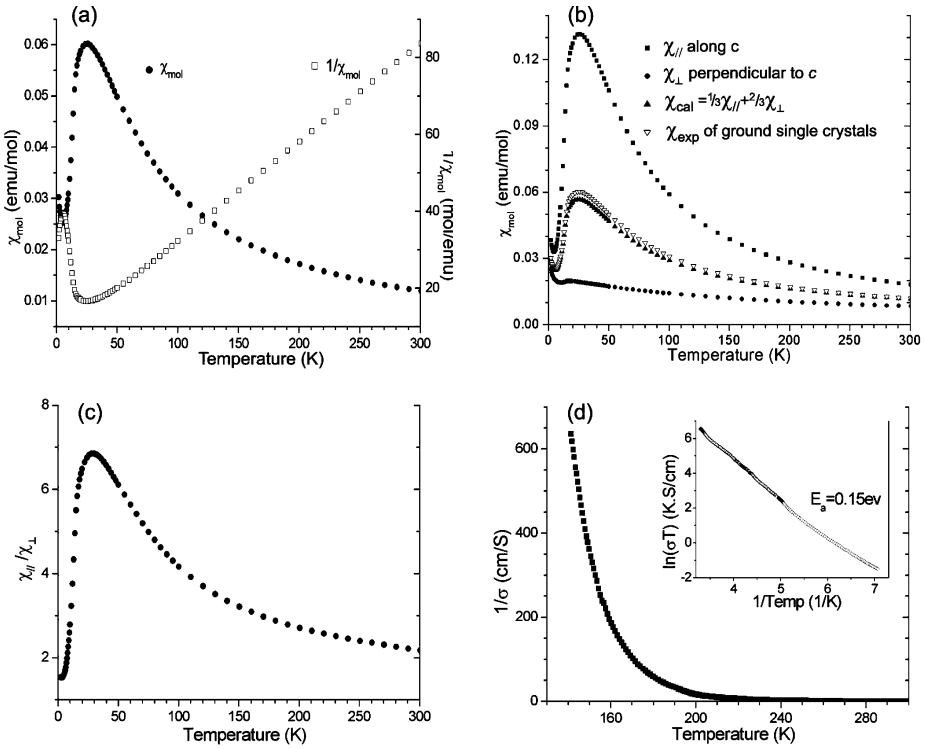

Figure 8. (a) Magnetic susceptibility and its inverse as a function of temperature for a sample finely ground from single crystals; (b) temperature dependence of the magnetic susceptibility of a single crystal of $Sr_6Co_5O_{14.70}$ along (■) and perpendicular (●) to the *c* axis; the powder susceptibility (▽) and the calculated random orientated single-crystal susceptibility (▲) by $\chi_{cal} = 1/3\chi + 2/3\chi_{\perp}$ are also shown in the figure for comparison; (c) temperature dependence of the magnetic anisotropy, defined as the ratio of the susceptibilities along and perpendicular to the *c* axis; (d) temperature dependence of the electric conductivity and the σT versus $1/T$ plot.

The charge distribution of the cobalt ions in a stoichiometric $Sr_6Co_5O_{15}$ can be either $3Co^{4+}(d^5) + 2Co^{3+}(d^6)$ or $4Co^{4+}(d^5) + 1Co^{2+}(d^7)$. According to the structure of $Sr_6Co_5O_{15}$ by Harrison et al.,[36] $4Co^{4+} + 1Co^{2+}$ might be a more suitable model because the polyhedral chain, 4Oh + TP, allows Co^{4+} and Co^{2+} to be located in different sites. A theoretic analysis on $Sr_6Co_5O_{15}$ by Whangbo et al.[45] suggested that the octahedral tetramer is nonmagnetic, while the single TP can be either $S = 1/2$ or $S = 3/2$. Largely due to the lack of phase-pure stoichiometric samples, their prediction has not yet confirmed by experiment. However, the observed effective moment (5.6 μ_B) of our single-crystal sample of $Sr_6Co_5O_{14.70}$ is significantly higher than what they expected. Here we are trying to understand the magnetic property based on the composite structure model. The polyhedral chain in $Sr_6Co_5O_{14.70}$ is a random composite of 4Oh + TP and 3Oh + 2IP; thus, the magnetic susceptibility should be the sum of these two components. For the 4Oh + TP polyhedral chain, we could take the spin-only value of $S = 3/2$ (3.87 μ_B) suggested by Whangbo et al.[45] For the 3Oh + 2IP chain, according to the increase of this component with the content of oxygen vacancies, one could expect that a hypothetical compound of $Sr_6Co_5O_{14}$ might have this structure. Therefore, the charge distribution might be $3Co^{4+} + 2Co^{2+}$, in which Co^{4+} occupies three Oh positions and Co^{2+} locates at two IP. For simplicity, we neglect the interaction between Oh and IP and assume that the 3Oh + 2IP chain can be considered as one octahedral trimer and two isolated IP. Due to the strong interaction of z^2 orbitals, the octahedral trimer has a single unpaired electron ($S = 1/2$). The splitting of the d orbitals in IP should be between the Oh and TP, so one would expect $S = 3/2$ for a Co^{2+} in IP. We could calculate the spin-only effective moment for the 3Oh + 2IP chain structure, $\mu_{cal} = 5.74\ \mu_B$. Considering the observed TP/IP ratio in the structure refinement, one obtains a sum of spin-only effective moment, $\mu_{cal} = 5.00\ \mu_B$. We should keep in mind that the above analysis neglected the spin−orbital coupling and the interaction between the Oh and IP. The spin−orbital coupling is quite strong for cobalt ions, which normally have $g > 2$, so the real effective moment should be larger than 5.00 μ_B. In addition, the Co2−Co3 distance in the structure of $Sr_6Co_5O_{14.70}$ is quite short (~2.49 Å) and a strong interaction of the z^2 orbitals is expected between TP and IP. It should also be noted that quantitative estimation of the magnetic property is difficult for the cobalt system. The actual magnetic interaction requires further study by using neutron diffraction at low temperature. Nevertheless, the above analysis did show that the structure model does not conflict with the result of the magnetic susceptibility measurements.

Figure 8d shows the electric resistivity ($1/\sigma$) along the *c* axis as a function of temperature. The $\ln(\sigma T)$ curve is also included in the figure. At room temperature, the resistivity along the *c* axis is small (~0.4 cm/S); it increases as the decrease of the temperature showing a semiconducting behavior. At the temperature lower than 140 K, the resistance

(45) Whangbo, M.-H.; Koo, H.-J.; Lee, K.-S.; Gourdon, O.; Evain, M.; Jobic, S.; Brec, R. *J. Solid State Chem.* **2001**, *160*, 239.

Table 8. 3-D Sections of the 4-D Superspace Group of $R\bar{3}m(00\gamma)0s$

$\gamma = p/k$	case 1	case 2	case 3
$p = 3n$, $k =$ even	$t = 0$ (mod. $1/k$)	$t = 1/(2k)$ (mod. $1/k$)	$t =$ arbitrary
3-D space group	$R\bar{3}c$	$R\bar{3}c$	$R3c$
$p = 3n$, $k =$ odd	$t = 0$ (mod. $1/(2k)$)	$t = 1/(4k)$ (mod. $1/(2k)$)	$t =$ arbitrary
3-D space group	$R\bar{3}$	$R32$	$R3$
$p \neq 3n$, $k =$ even	$t = 0$ (mod. $1/(3k)$)	$t = 1/(6k)$ (mod. $1/(3k)$)	$t =$ arbitrary
3-D space group	$P\bar{3}$c	$P\bar{3}c$	$P3c$
$p \neq 3n$, $k =$ odd	$t = 0$ (mod. $1/(6k)$)	$t = 1/(12k)$ (mod. $1/(6k)$)	$t =$ arbitrary
3-D space group	$P\bar{3}$	$P32$	$P3$

is too high to be measured by the current instrumentation. The conductivity follows Arrhenius law in the temperature range 140−300 K. The $\ln(\sigma T)$ versus $1/T$ plot shown in Figure 8d leads to an activation energy of about $E_a = 0.15$ eV, which may correspond to the hopping energy of the electron along the polyhedral chains.

Conclusion

$Sr_6Co_5O_{15}$ is a unique member in the 2H-perovskite-related oxides. Although many investigations were devoted to this compound, the study on oxygen-deficient single crystals shows that the structure and magnetic properties of this compound are much more complicated than expected. One of the interesting findings of the present study is that large single crystals can be readily grown in the basic flux of K_2CO_3 in the presence of a few transition metal oxides, Cr_2O_3, MnO_2, or NiO. Although the reaction mechanism has not yet been fully understood, the presence of the high oxidation chromate and permanganate ions in the flux suggests that the assistance to the oxidation of cobalt ions is required in this reaction system.

Unlike the other known 2H-perovskite related oxides, in which the polyhedral chains are all composed of octahedra and trigonal prisms, the structure of $Sr_6Co_5O_{14.70}$ and $Sr_6Co_{4.9}Ni_{0.1}O_{14.36}$ consists of polyhedral chains repeat of three Oh and two IP. Such a polyhedral chain is related to that in $Sr_6Rh_5O_{15}$ by shifting of the O_3 triangles along the c axis accompanied by a rotation of about 30°. Three observations suggest that this unique polyhedral chain may have a general impact to the structural principle of the 2H-peroskite-related oxides. First, mapping of the known 2H-perovskite-related oxides in shifting of the O_3 triangle ($2\Delta z/c_{perov}$) and the rotation angle (Θ) reveals a correlating trend that represents a gradual transformation from TP to IP. Second, the O3 atom in both $Sr_6Co_5O_{14.70}$ and $Sr_6Co_{4.9}Ni_{0.1}O_{14.36}$ can be described by two independent positions, corresponding to the polyhedral chain consisting of random composite of 4Oh + TP and 3Oh + 2IP. These two components depend on the content of oxygen vacancies in the structure, i.e., the more the oxygen vacancies, the higher the 3Oh + 2IP component will be. This explains the $Sr_6Co_5O_{15}$ structure observed for the powder sample by Harrison et al. Finally the 3-D space groups of these two structure types, i.e., $R32$ for $Sr_6Rh_5O_{15}$ and $R\bar{3}$ for $Sr_6Co_5O_{14.70}$, are the subgroups of a 4-D superspace group, $R\bar{3}m(00\gamma)0s$; both $Sr_6Rh_5O_{15}$ and $Sr_6Co_5O_{14.70}$ can be described as commensurate modulated structures in this 4-D superspace formalism in different 3-D sections, i.e., different t-phases. Another implication of the structure relationship between $Sr_6Rh_5O_{15}$ and $Sr_6Co_5O_{14.70}$ is that the other possible t-phases listed in Table 8 may also be meaningful for the 2H-perovskite-related oxide family.

The magnetic property of $Sr_6Co_5O_{14.70}$ can be understood in the frame of the random composite structure model. One of the assumptions is that the Co^{4+} ions are all located in Oh and the Co^{2+} ions are located at either TP or IP in the structures. Although at present there is no direct experimental evidence confirming such charge distribution, the analysis based on this assumption can be used to interpret the magnetic susceptibility data. Additionally, the measurement also shows high conductivity around room temperature and small activation energy for $Sr_6Co_5O_{14.70}$ sample along the c axis, indicative of a low hopping barrier of electrons along the polyhedral chains.

Acknowledgment. We thank the financial support from NSFC (20371005 and 20221101) and Prof. Song Gao and Prof. Yan Zhang at PKU for magnetic and conductive measurements.

Supporting Information Available: Atomic parameters of $Sr_6Co_{4.9}Ni_{0.1}O_{14.36}$ in a 4-D superspace formalism approach. This material is available free of charge via the Internet at http://pubs.acs.org.

IC060862M